

Dinuclear Cu(II) Complexes of Isomeric Bis-(3-acetylacetonate)benzene Ligands: Synthesis, Structure, and Magnetic Properties

Marzio Rancan,^{*,†} Alessandro Dolmella,[‡] Roberta Seraglia,[†] Simonetta Orlandi,^{§,||} Silvio Quici,^{*,§,||} Lorenzo Sorace,[⊥] Dante Gatteschi,[⊥] and Lidia Armelao^{*,†}

[†]Istituto di Scienze e Tecnologie Molecolari (ISTM), Consiglio Nazionale delle Ricerche (CNR) and Consorzio Interuniversitario per la Scienza e Tecnologia dei Materiali (INSTM), Dipartimento di Scienze Chimiche, Università di Padova, Via F. Marzolo, 1-35131, Padova, Italy

[‡]Dipartimento di Scienze Farmaceutiche, Università di Padova, Via F. Marzolo, 5-35131, Padova, Italy

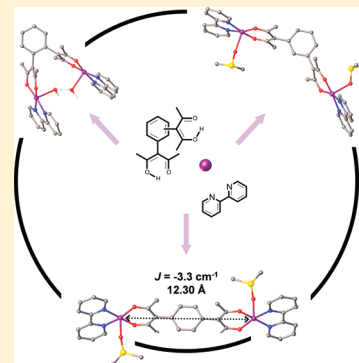
[§]Istituto di Scienze e Tecnologie Molecolari (ISTM), Consiglio Nazionale delle Ricerche (CNR), Via C. Golgi, 19-20133, Milano, Italy

^{||}Polo Scientifico e Tecnologico (PST), Consiglio Nazionale delle Ricerche (CNR), via Fantoli, 16/15-20138, Milano, Italy

[⊥]Dipartimento di Chimica "U. Schiff" and Consorzio Interuniversitario per la Scienza e Tecnologia dei Materiali (INSTM), Università di Firenze, Via della Lastruccia 3-13, 50019, Sesto Fiorentino, Firenze, Italy

Supporting Information

ABSTRACT: Highly versatile coordinating ligands are designed and synthesized with two β -diketonate groups linked at the carbon 3 through a phenyl ring. The rigid aromatic spacer is introduced in the molecules to orient the two acetylacetonate units along different angles and coordination vectors. The resulting *para*, *meta*, and *ortho* bis-(3-acetylacetonate)-benzene ligands show efficient chelating properties toward Cu(II) ions. In the presence of 2,2'-bipyridine, they promptly react and yield three dimers, 1, 2, and 3, with the bis-acetylacetonate unit in bridging position between two metal centers. X-ray single crystal diffraction shows that the compounds form supramolecular chains in the solid state because of intermolecular interactions. Each of the dinuclear complexes shows a magnetic behavior which is determined by the combination of structural parameters and spin polarization effects. Notably, the *para* derivative (1) displays a moderate antiferromagnetic coupling ($J = -3.3 \text{ cm}^{-1}$) along a remarkably long Cu...Cu distance (12.30 Å).



INTRODUCTION

The coordination properties of β -diketones have been under investigation for a long time as simple and highly efficient metal chelating. By linking two β -diketone groups through suitable spacers, highly versatile ligands can be obtained. Various studies have been mainly devoted to 1,3- and 1,4-aryl bis- β -diketone derivatives bonded through carbon atoms 1 and 5 of the β -diketone groups. For instance, Lindoy and co-workers have developed an interesting coordination chemistry which produced metal dimers, triangles, and tetrahedra¹ based on aryl bis- β -diketone ligands and metal ions of the first transition series.

In general, the chemistry of mono- and bis-3-substituted β -diketones is less rich in comparison to that of the 1,5-substituted derivatives. Recently, a survey on the synthetic routes of 3-substituted 2,4-pentadionate ligands and their application as photoactive systems has been published.² In this framework, we have recently addressed our interest to bis-acetylacetonate ligands with the two β -diketone units linked to a phenyl ring through the carbon 3 at the 1,4-, 1,3- and 1,2-atoms. This leads to a series of three bis-(3-acetylacetonate)benzene

compounds, named *para* (*p*-LH₂), *meta* (*m*-LH₂), and *ortho* (*o*-LH₂) isomers (Figure 1).

The presence of the rigid aromatic spacer in such systems represents a peculiar aspect, since it allows to orient the two acetylacetonate units along different angles and coordination vectors in the three isomers. This paves the way, still unexplored, for the exploitation of these ligands in the design and synthesis of a variety of compounds ranging from discrete molecular cages and molecular boxes (i.e., dimers, triangles, squares, and polyhedral capsules) to metal coordination polymers and networks, up to surface-assisted coordination chemistry reactions.

Very few examples of metal complexes with the bis-(3-acetylacetonate)benzene ligands are described in the literature.^{3–6} Maverick et al. reported a copper molecular square³ [Cu(*m*-L)]₄ endowed with interesting H₂ sorption properties and able to host a fullerene molecule in its cavity. Similarly, a first work reported that the *o*-LH₂ isomer leads to a copper

Received: February 20, 2012

Published: April 19, 2012



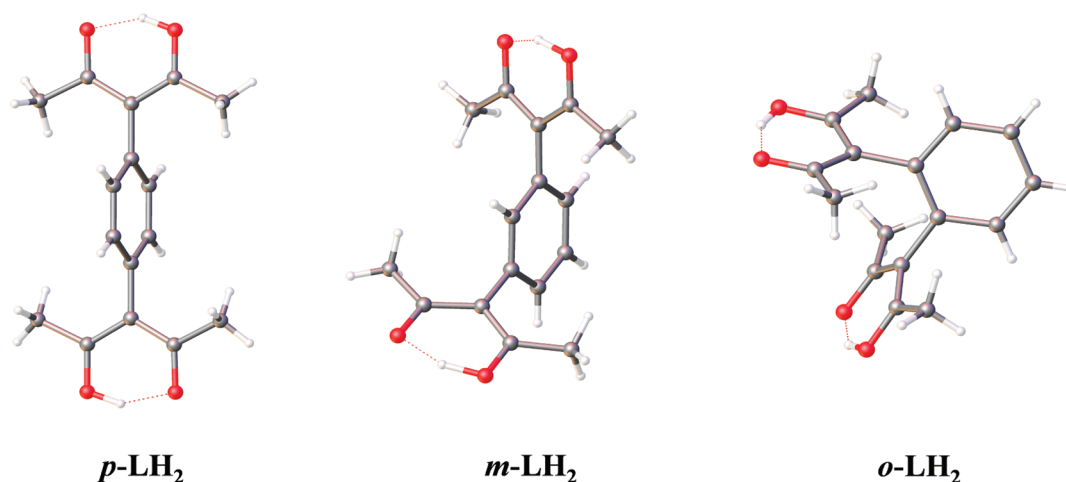


Figure 1. Three bis-(3-acetylacetonate)benzene isomers: *p*-LH₂, *m*-LH₂, and *o*-LH₂. Color code: O red, C gray, H white, H bonds dashed red lines.

Table 1. Crystal Data and Details of Data Collections

compound	<i>p</i> -LH ₂	<i>o</i> -LH ₂	1	2	3
chemical formula	C ₁₆ H ₁₈ O ₄	C ₁₆ H ₁₈ O ₄	C ₄₀ H ₄₄ Cl ₂ Cu ₂ N ₄ O ₁₄ S ₂	C ₄₄ H ₅₆ Cl ₂ Cu ₂ N ₄ O ₁₆ S ₄	C ₄₅ H ₅₄ Cl ₂ Cu ₂ N ₄ O ₁₇
formula mass	274.30	274.30	1066.93	1223.15	1120.90
crystal system	orthorhombic	monoclinic	triclinic	triclinic	orthorhombic
<i>a</i> /Å	13.2257(3)	17.7839(1)	11.0255(3)	12.3340(6)	20.1413(2)
<i>b</i> /Å	12.6283(3)	8.5189(3)	11.1307(3)	13.2732(5)	17.7925(2)
<i>c</i> /Å	8.7883(2)	11.8682(8)	12.0879(3)	18.358 (1)	28.3123(3)
α /deg	90.00	90.00	104.425(2)	78.327(4)	90.00
β /deg	90.00	124.45(1)	103.075(2)	81.739(4)	90.00
γ /deg	90.00	90.00	108.667(2)	64.461(4)	90.00
unit cell volume/Å ³	1467.80(6)	1482.7(2)	1283.20(6)	2650.3(2)	10146.1(2)
temperature/K	298(1)	298(1)	123(1)	140(1)	150(1)
space group	<i>Pnma</i>	<i>C12/c1</i>	<i>P</i> $\bar{1}$	<i>P</i> $\bar{1}$	<i>Pbca</i>
<i>Z</i>	4	4	1	2	8
$\rho_{\text{calc}}/\text{mg mm}^{-3}$	1.241	1.229	1.381	1.533	1.468
μ/mm^{-1}	0.505	0.499	1.076	3.988	2.630
crystal size/mm ³	0.05 × 0.05 × 0.40	0.35 × 0.40 × 0.55	0.70 × 0.30 × 0.12	0.20 × 0.06 × 0.06	0.30 × 0.20 × 0.20
radiation type	Cu K α	Cu K α	Mo K α	Cu K α	Cu K α
<i>R</i> ₁ , <i>wR</i> (<i>F</i> ²) (<i>I</i> > 2 σ (<i>I</i>)) ^a	0.0456, 0.1316	0.0543, 0.1659	0.0353, 0.1023	0.0718, 0.2164	0.0595, 0.1605
<i>R</i> ₁ , <i>wR</i> (<i>F</i> ²) (all data) ^a	0.0512, 0.1389	0.0576, 0.1721	0.0480, 0.1057	0.0829, 0.2240	0.0673, 0.1672

^a*R*₁ = ($\sum ||F_o| - |F_c|| / \sum |F_o|$); *wR*₂ = $\{\sum [w(F_o^2 - F_c^2)^2] / \sum [w(F_o^2)^2]\}^{1/2}$; GOF = $\sum [w(F_o^2 - F_c^2)^2] / (n - p)\}^{1/2}$ where *n* is the number of data and *p* is the number of parameters refined.

dimer [Cu(*o*-L)]₂.⁴ Recently, we showed that the reaction between *o*-LH₂ and Cu²⁺ generates a dimer–trimer *constitutional dynamic library*⁶ ([Cu(*o*-L)]_{*n*}, *n* = 2, 3) where the designed introduction of a well suited guest (hexamethylenetetramine, hmt) allowed us to orchestrate the system. The hmt molecule acts as an external stimulus for self-sorting of the system toward the supramolecular triangle {[Cu(*o*-L)]₃C(hmt)}. These findings fostered us to systematically study the coordination properties of the bis-(3-acetylacetonate)benzene isomers toward Cu(II) ions in the presence of a second chelating nitrogen-based ligand, that is, 2,2'-bipyridine. Under these conditions the three ligands (*p*-LH₂, *m*-LH₂, and *o*-LH₂) yield a series of dinuclear copper complexes (1, 2, and 3) with similar composition. The compounds have been fully characterized by X-ray single crystal diffraction and Electrospray Ionization (ESI) mass spectrometry. Structural data show an analogue square pyramidal coordination around Cu(II) ions, with the β -diketonate ligands lying in bridging position between the two

metal centers. The magnetic behavior of metal complexes based on the three bis-(3-acetylacetonate)benzene ligands is here investigated for the first time. Notably, compound 1 shows a moderate antiferromagnetic coupling (*J* = −3.3 cm^{−1}) along a remarkable Cu...Cu distance (12.30 Å). Magnetic measurements evidence that each of the three dinuclear complexes is characterized by a magnetism that can be correlated to the combination of structural parameters and ligand *spin polarization* effects.

EXPERIMENTAL SECTION

Synthesis. We report here the general procedure for the preparation of compounds 1–3. Detailed synthesis of ligands (*p*-LH₂, *m*-LH₂, and *o*-LH₂) and dinuclear Cu (II) complexes (1–3) is described in the Supporting Information. To a methanol solution (50 mL) of copper perchlorate (185 mg, 0.5 mmol), solid 2,2'-bipyridine (78 mg, 0.5 mmol) was added in small portions. The mixture was stirred for 2 h, and LH₂ (69 mg, 0.25 mmol) in methanol (10 mL) was added dropwise. In the case of 1 and 2, the obtained solid has been filtered, washed, and recrystallized. Compound 3 is characterized by a

higher solubility: the obtained solution has been refluxed overnight, the solvent removed in vacuum, and the obtained solid washed and recrystallized.

ESI/MS Spectrometry. The ESI mass spectra were obtained using a LCQ DECA ion trap instrument (ThermoFisher Scientific, San José, CA, U.S.A.), operating in positive ion mode. The entrance capillary temperature was 280 °C and the capillary voltage was 5 kV. Compounds 1–3 were first dissolved in dimethylsulfoxide (DMSO) and then diluted in acetonitrile to obtain a 10^{-6} M concentration. The acetonitrile solutions of each compound were introduced into the ESI ion source by direct infusion at a flow rate of 10 μ L/min. The He pressure inside the trap was kept constant. The pressure directly read by ion gauge (in the absence of the N₂ stream) was 2.8×10^{-5} Torr.

X-ray Structure Determination and Refinement. Single crystals were fastened on the top of a Lindemann glass capillary or mounted using Paratone-N oil and centered on the head of a four-circle kappa goniometer Oxford Diffraction Gemini E diffractometer, equipped with a 2K \times 2K EOS CCD area detector and sealed-tube Enhance (Mo) and (Cu) X-ray sources. Data were collected by means of the ω -scans technique using graphite-monochromated radiation, in a 1024 \times 1024 pixel mode, using 2 \times 2 pixel binning. The diffraction intensities were corrected for Lorentz/polarization effects as well as with respect to absorption. Empirical multi-scan absorption corrections using equivalent reflections were performed with the scaling algorithm SCALE3 ABSPACK. Data collection, data reduction and finalization and cell refinement were carried out through the CrysAlisPro software (CrysAlisPro, Oxford Diffraction Ltd., Version 1.171.34.36). Accurate unit cell parameters were obtained by least-squares refinement of the angular settings of 1326 (*p*-LH₂), 2407 (*o*-LH₂), 33245 (1), 6540 (2), and 14560 (3) strongest reflections, chosen from the whole experiment. Structures were solved by means of direct methods using SHELXS⁷ and refined by full-matrix least-squares methods based on F_o^2 with SHELXL-97⁷ in the framework of OLEX2⁸ software. In the last cycles of refinement, ordered non-hydrogen atoms were refined anisotropically whereas disordered partial occupancy non-hydrogen atoms were refined isotropically. Hydrogen atoms connected to carbon atoms were included in idealized positions, and a riding model was used for their refinement. A summary of the crystallographic data and of the refinement parameters for each compound is provided in Table 1. Crystal structure determination and refinement details for each compound are instead reported in the Supporting Information, that also includes ORTEP plots and structure description for ligands *p*-LH₂ and *o*-LH₂. Bond lengths and angles of the metal coordination spheres, along with ORTEP plots, for compounds 1, 2, and 3 are reported in the Supporting Information (Table S3). CCDC 854278 (*p*-LH₂), CCDC 854279 (*o*-LH₂), CCDC 854280 (1), CCDC 854281 (2) and CCDC 854282 (3) contain the supplementary crystallographic data for this paper. These data can be obtained free of charge from the Cambridge Crystallographic Data Center via www.ccdc.cam.ac.uk/data_request/cif.

Magnetism. The magnetic susceptibilities of the powdered samples were measured with a Cryogenic SQUID S600 magnetometer in the 2–300 K temperature range, with an applied field of 1.0 T ($T > 30$ K) and 0.1 T ($T < 30$ K). The raw data were corrected for the underlying sample holder contribution and the intrinsic diamagnetism of the sample estimated by the Pascal's constants.

RESULTS AND DISCUSSION

Synthesis. The *p*-LH₂, *m*-LH₂, and *o*-LH₂ bis-(3-acetylacetonate)benzene ligands have been prepared according to the procedure reported by Ramirez and co-workers (Figure 2).⁹

Reaction of two moles of 2,2,2-trimethoxy-4,5-dimethyl-1,3-dioxaphospholene¹⁰ (A) with a mole of the corresponding bis-aldehyde (B) dissolved in CH₂Cl₂ under rigorous nitrogen atmosphere afforded the bis-pentaoxyphosphorane intermediate (C) as a diastereomeric mixture. The intermediate C was

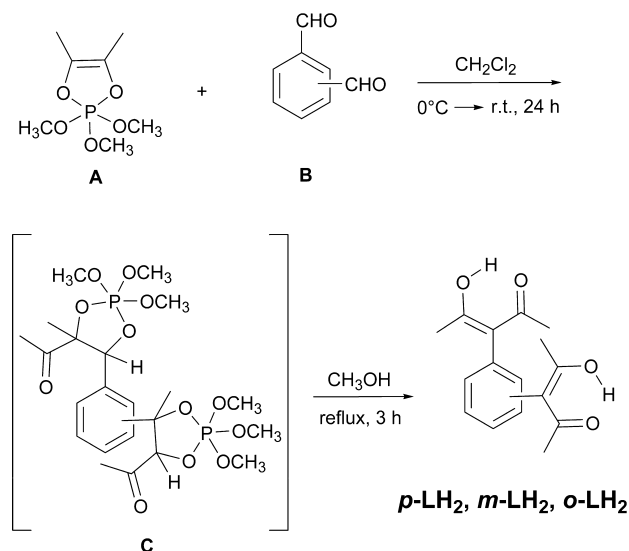
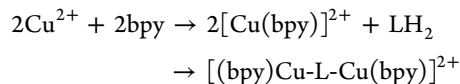


Figure 2. Synthesis of the ligands.

directly hydrolyzed under reflux in CH₃OH to give *p*-LH₂, *m*-LH₂, and *o*-LH₂ ligands in 80, 50, and 25% yield, respectively. It has to be stressed that while in the case of terephthalaldehyde (*p*-dialdehyde) and isophthalaldehyde (*m*-dialdehyde) the only obtained product from the methanolysis of C is the tetraketone in the dienol form, in the case of phthalaldehyde (*o*-dialdehyde) both the dienol and the monoenoletriketone products are formed.⁹ In this last case the pure *o*-LH₂ ligand can be obtained by careful crystallization of the product, although this lowers the reaction yield. Single crystal X-ray measurements show that in the solid state the two acetylacetonate groups are in the *cis*-enol form in all the three isomeric ligands (Figure 1). The *m*-LH₂ X-ray structure has been previously determined³ while the *p*-LH₂ and *o*-LH₂ ones are here reported for the first time. Moreover it has been evidenced that the O–H...O are involved in strong H-bonds, and that the O...O distances are in the narrow 2.43–2.46 Å interval.

Reaction of *m*-LH₂ and *o*-LH₂ with Cu(II) leads to compounds of formula [CuL]_{*n*}, that is, a dimer,⁴ a molecular triangle,⁶ and a molecular square³ for *n* = 2, 3, and 4, respectively. These compounds are very soluble in organic solvents as CH₂Cl₂ and CHCl₃. On the other hand, because of its geometry, the *p*-LH₂ ligand forms an insoluble product, probably a one-dimensional (1D) coordination polymer. To prevent the formation of the insoluble coordination polymer, an ancillary bidentate coligand (i.e., tetramethylethylenediamine, 2,2'-bipyridine and 1,10-phenanthroline) has been introduced⁵ and the same strategy was also adopted for the meta and ortho ligands. The synthesis route is reported below: a Cu(ClO₄)₂ solution (methanol) is first reacted with 2,2'-bipyridine (bpy) in a equimolar amount and subsequently a ligand solution (methanol) is added (molar ratio Cu:L = 2:1).



Three dinuclear copper complexes of formula {[*(bpy)*Cu(*sol*)]₂(L)}(ClO₄)₂ (1, 2, and 3 with the ligand *p*-LH₂, *m*-LH₂, and *o*-LH₂, respectively) have been obtained in almost quantitative yields. Elemental analysis suggests that in the as prepared compounds the *sol* moieties are water molecules. Interestingly, the reaction works very well without using any

base to deprotonate the acetylacetonate groups, the reaction driving force being probably the high affinity of the acetylacetonate oxygen atoms for Cu(II) ions. In the case of **1** and **2**, the product insolubility in the reaction medium plays an important role too. We found that in methanol and in the absence of a base the yields are higher compared to data previously reported using the *para* substituted ligand in the presence of NaOH.⁵ The solubility in organic media of the three products increases from **1** to **3**. Dimer **1** is soluble only in high coordinating solvents such as DMSO, DMF, and pyridine; dimer **2** is soluble in the same solvents and in acetonitrile, while compound **3** is very soluble in organic solvents such as acetonitrile, acetone, and methanol.

ESI/MS Spectrometry. ESI/MS analysis of compounds **1**–**3** show similar spectra (see for instance the ESI-MS positive ion mode spectra of compound **3**, Figure 3). The most abundant

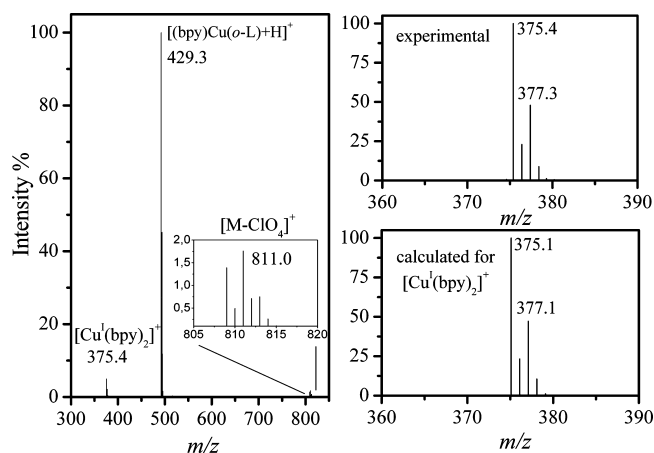
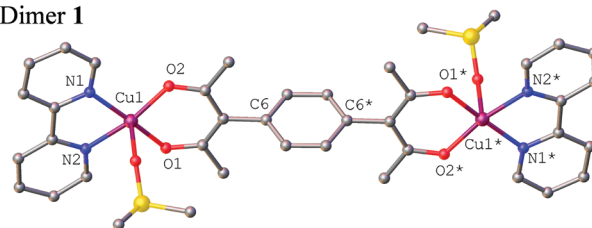


Figure 3. ESI-MS positive ion mode spectra of compound **3** (right); experimental and calculated $[\text{Cu}^{\text{I}}(\text{bpy})_2]^+$ peak (left).

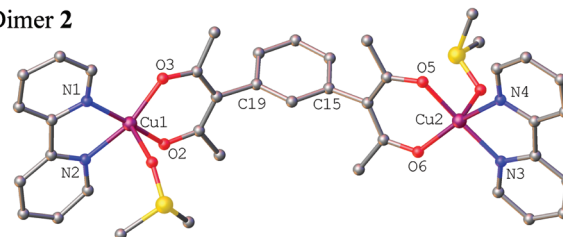
peak is due to the ionic species $[(\text{bpy})\text{Cu}(\text{L})+\text{H}]^+$ ($m/z = 492$); for **2** and **3**, the molecular cation $[\text{M}-\text{ClO}_4]^+$ is observed at $m/z = 810$ with a very low abundance (ca. 3%). The presence of a low abundant ion at $m/z = 375$ has been detected for all the three dimers (5–15%). It can be ascribed to the ionic species $[\text{Cu}^{\text{I}}(\text{bpy})_2]^+$ where the metal ion has been reduced to Cu(I). This reduction behavior has already been described in literature for Cu(II) pyridil chelates. In particular, Gianelli and co-workers¹¹ have shown as this process derives from a charge transfer between the solvent and the metal complex in the gas phase. It is worthwhile recalling that the electrospray source can be considered as a particular electrolytic cell, in which electrolysis maintains the charge balance allowing the continuous production of charged droplets.¹²

Structure Description. For compounds **1**–**3** single crystals have been isolated and structurally characterized (Figure 4). The general formula of the dimers is $\{[(\text{bpy})\text{Cu}(\text{sol})]_2(\text{L})\}(\text{ClO}_4)_2$, where *sol* is a DMSO (**1** and **2**) or a water (**3**) molecule; bis-(3-acetylacetonate)benzene ligands are bridging between the two metal centers. The Cu(II) ions show a square pyramidal coordination in compound **2**, whereas in compound **1** and **3**, because of intermolecular interactions (see below), the metal environment can be described as pseudo-octahedral. In all compounds the Cu(II) ions are surrounded by two acetylacetonate oxygen and two bipyridil nitrogen atoms in the equatorial plane, with an apical position held by a solvent molecule. In the compounds showing pseudo-octahedral

Dimer 1



Dimer 2



Dimer 3

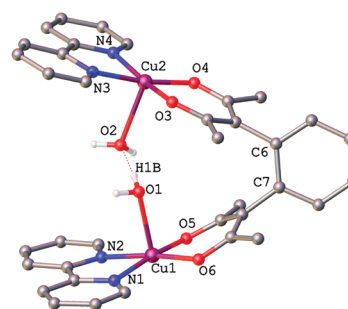
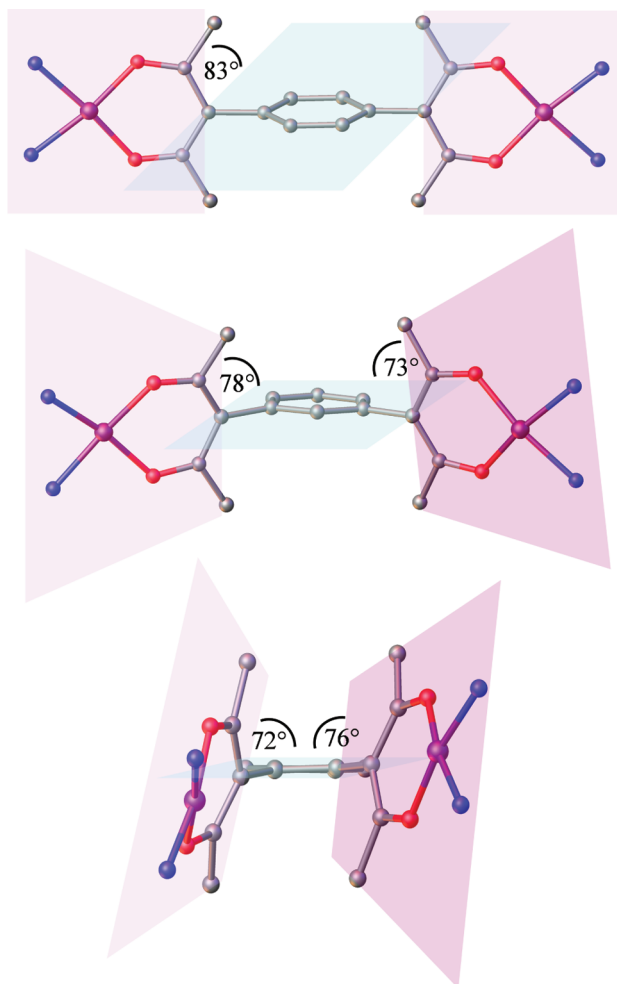


Figure 4. Compounds **1**, **2**, and **3**. Color code (applied to the following figures): Cu purple, S yellow, O red, N blue, C gray, H-bond dashed red line. H atoms and ClO_4^- anions are omitted for clarity.

coordination the sixth position is occupied by a nitrogen atom of the closest nearby bipyridine molecule, with a long Cu...N interaction (ca. 3.3 Å for **1** and ca. 3.2 Å for **3**). The Cu–O_{acac} and Cu–N_{bpy} distances are in the intervals 1.890–1.927 Å and 1.980–2.004 Å, respectively (Table 2). The crystal structure of compound **1** has been already reported;⁵ below we point to some features useful for the following structural-magnetochemical correlations. The two copper atoms lie at 12.30 Å. The equatorial plane, formed by the acetylacetonate oxygen and the bipyridyl nitrogen atoms around each metal ion is nearly orthogonal (83°) to the plane of the acetylacetonate phenyl ring (Figure 5). Finally, the torsional angle $\angle \text{Cu1}-\text{C6}-\text{C6}^*-\text{Cu1}^*$ (* = $-x, -y, 1-z$) is 0° by symmetry (Figure 4). The copper coordination sphere in compound **2** is similar to the one found in dimer **1**. Two DMSO molecules, oriented in antiparallel fashion, occupy the apical position of the coordination sphere (Cu–O_{DMSO}: 2.229 and 2.259 Å). The two copper atoms are at a distance of 11.55 Å and the $\angle \text{Cu1}-\text{C19}-\text{C15}-\text{Cu2}$ torsional angle is 13.4° (Figure 4). Moreover, the plane of the acetylacetonate phenyl ring define angles of 78° and 73°, respectively (Figure 5). Unlike compounds **1** and **2**, the two copper atoms of **3** are cofacial (Cu...Cu distance 5.68 Å), likely because of the H-bond between the two apical water molecules. Compound **3** has a strained tweezers folding, with a torsional angle $\angle \text{Cu1}-\text{C7}-\text{C6}-\text{Cu2}$ of 12.2° (Figure 4). The equatorial coordination of the Cu ions is the same as in **1** and **2**, while the apical positions are taken by two water molecules (Cu–O_w: 2.235 and 2.321 Å) involved in a H-bond interaction (O1–H1B...O2: 1.876 Å; O1...O2: 2.74 Å). These

Table 2. Selected Bond Lengths (Å) for 1, 2, and 3

1		2		3	
Cu1–O1	1.9173(7)	Cu1–O2	1.898(5)	Cu2–O5	1.891(5)
Cu1–O2	1.9003(7)	Cu1–O3	1.909(5)	Cu2–O6	1.926(5)
Cu1–N2	1.9888(7)	Cu1–N1	1.998(6)	Cu2–N3	1.980(6)
Cu1–N1	2.0014(8)	Cu1–N2	2.002(6)	Cu2–N4	2.005(6)
				Cu1–O5	1.910(2)
				Cu1–O6	1.893(2)
				Cu2–O3	1.900(2)
				Cu2–O4	1.894(2)
				Cu2–N4	1.998(3)
				Cu2–N3	1.998(3)
				O1–H1B...O2	1.876, 175.21

Figure 5. Orientation of the “CuO₂N₂” mean planes and the phenyl plane in compounds 1, 2, and 3.

two water molecules are also involved in further H-bonds with three crystallization acetone molecules (Supporting Information, Figure S6). As for compound 2, the copper ions equatorial planes and the plane of the phenyl ring deviate appreciably from orthogonality (angles: 76° and 72° respectively, Figure 5).

All the three compounds exhibit noncovalent intermolecular interactions in the solid state (Figure 6) leading to supramolecular chains. In 1 and 3, intermolecular interactions are very similar and involve the acetylacetonate moiety of a molecule and the bipyridine of the closest nearby molecule (distances: ca. 3.1 Å in 1 and ca. 3.2 Å in 3; Figure 6b and d). This interaction is responsible of the pseudo-octahedral environment found in both 1 and 3 complexes (see above). In 2, the supramolecular chains are stabilized by a proper $\pi\cdots\pi$ stacking (I, distance 3.3–3.4 Å; Figure 6e and f) and by a weaker interaction (II, distance 3.4–3.5 Å; Figure 6e and g),

both of them involving the bipyridine ligands of two nearby molecules

Magnetic Behavior. Magnetic studies have been pursued on the three dimers. The plot of χT vs T (Figure 7a) for complex 1 clearly shows moderate antiferromagnetic interactions with a decrease, below 50 K, from the room temperature value of 0.8 emu K mol^{−1} (as expected for two independent $S = 1/2$ with $g > 2.00$) to 0.2 emu K mol^{−1} at 2 K. The experimental curve can be fitted by a Bleaney–Bowers equation,¹³ based on the Hamiltonian $H = -JS_1S_2 + g\beta\mathbf{B}\cdot\mathbf{S}$, providing the following best fit parameters: $J = -3.30 \pm 0.02$ cm^{−1}, $g = 2.060 \pm 0.002$ ($R^2 = 0.99846$). In addition, the χ vs T (Figure 7b) curve shows a maximum at 2.9 K which provides a similar $|J|$ value (≈ 3.3 cm^{−1}) by applying the relation $|J| \approx kT_{\max}/0.6$ (k is the Boltzmann constant and T_{\max} the temperature at the χ maximum). The magnitude of the singlet–triplet gap, and thus of the antiferromagnetic intradimer interaction, was confirmed by the field dependence of the magnetization at low temperature (2 K), clearly revealing a field induced spin state change (singlet \rightarrow triplet) close to $B = 3.5$ T. The corresponding maximum of $\partial M/\partial B$ vs B curve is evidenced in the inset of Figure 7a.

Much weaker magnetic interactions among the two copper centers were observed for 2 and 3, both showing very regular Curie–Weiss plots. In particular for 2 the χT vs T plot (Figure 8) suggested a very weak ferromagnetic interaction, with χT feebly increasing above the expected Curie value below 20 K, and a subsequent drop. This interpretation was confirmed by a fit of the corresponding Curie–Weiss plot (inset of Figure 8), which provided a positive (ferromagnetic) Weiss constant of 1.3 K and a Curie constant of 0.78 emu K mol^{−1}.

As for 3, temperature dependent magnetic data clearly points to the presence of negligible exchange coupling interaction, χT value being constant down to 10 K at 0.8 emu K mol^{−1}, in agreement with two essentially uncoupled Cu(II) centers (Figure 9). Accordingly, the fit of the corresponding Curie–Weiss plot (inset Figure 9) provides a Curie constant of $C = 0.80$ emu K mol^{−1} and a negative (antiferromagnetic) θ value of 0.12 K, confirming the weakness of the interaction.

As described above, compound 1 displays a moderate antiferromagnetic coupling which occurs along a remarkably long Cu \cdots Cu distance (12.30 Å). This is one of the few examples of dinuclear copper compounds where the magnetic coupling is still not negligible at distances longer than 1 nm.¹⁴ The J value (-3.3 cm^{−1}) is comparable to previous data for other dinuclear copper systems with π -conjugated bridging ligands such as aromatic diamines (Cu \cdots Cu = 12.07 Å, $J = -3.2$ cm^{−1}; ^{14a} Cu \cdots Cu = 12.26 Å, $J = -8.5$ cm^{−1}; ^{14f} Cu \cdots Cu = 16.42 Å, $J = -2.0$ cm^{−1}; ^{14f}) and bis(oxamate) with an aromatic spacer (Cu \cdots Cu = 10.80 Å, $J = -2.2$ cm^{−1}; ^{14d} Cu \cdots Cu = 12.20 Å, $J = -8.7$ cm^{−1}; ^{14e} Cu \cdots Cu = 14.95 Å, $J = -3.9$ cm^{−1}; ^{14g}). Probably, the most intriguing result of the magnetic studies is the exchange coupling trend along the series of the three dinuclear copper complexes. A rationalization of the different magnetic

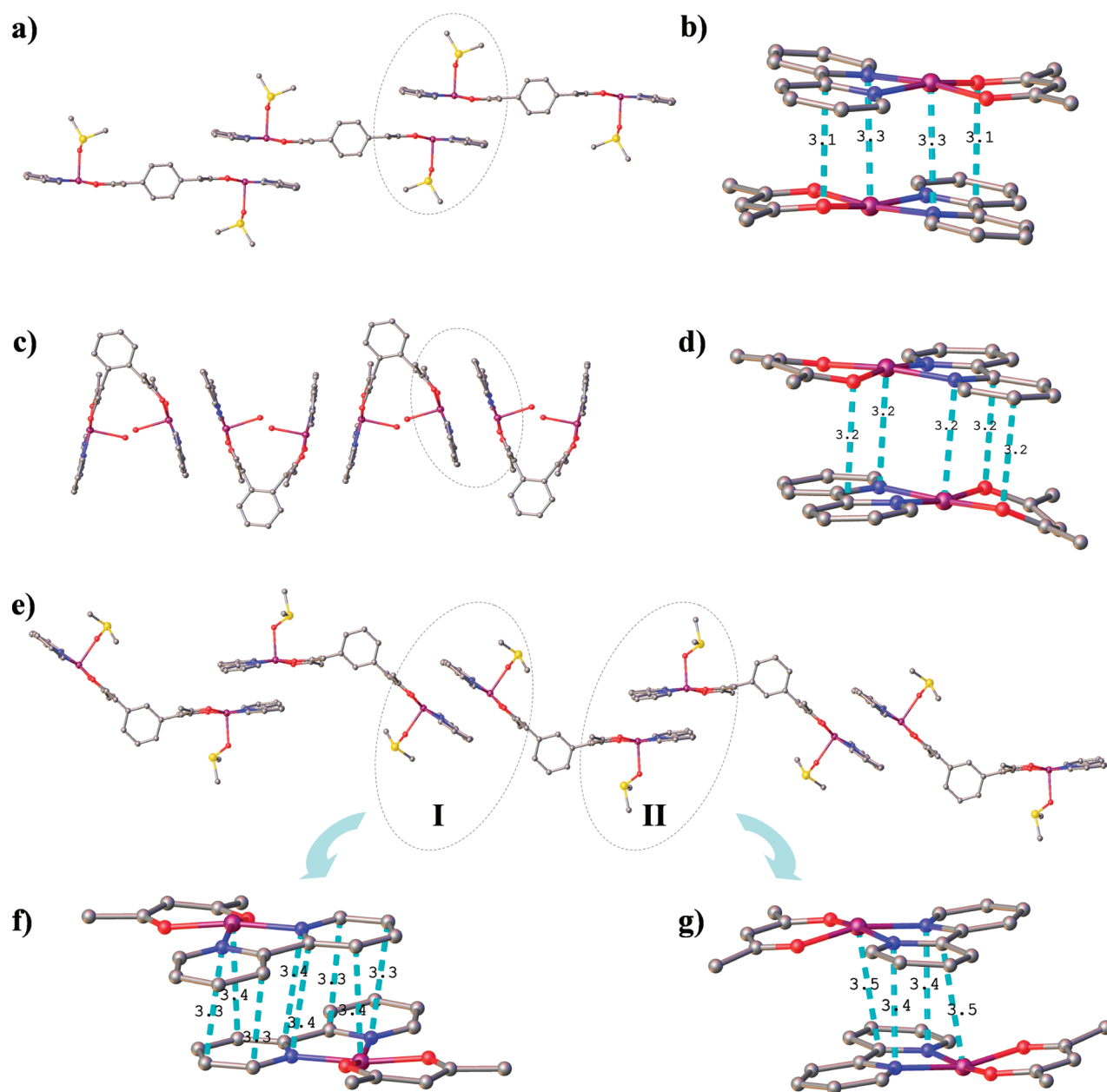


Figure 6. Supramolecular chains. Compound 1 (a), 3 (c), 2 (e), and their intermolecular interactions 1 (b), 3 (d), 2 (f: I; g: II). Dotted cyan lines: intermolecular interactions (Å). H atoms, ClO_4^- anions, and coordinating solvent molecules (in b, d, f, and g) are omitted for clarity.

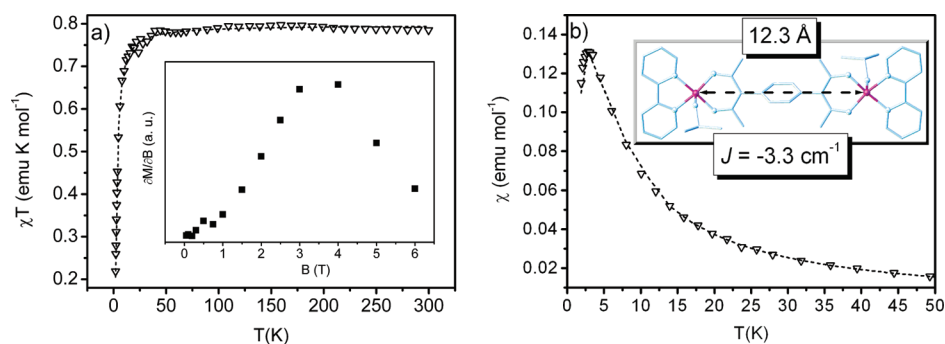


Figure 7. χT vs T (in the 0–300 K range) and χ vs T (in the 0–50 K range) plots for complex 1 (empty triangles) and best fit curve (dashed line). In the inset of 7a, the derivative of the isothermal magnetization curve (2 K) with respect to the field is reported, evidencing a field induced spin state crossing at around 3.5 T.

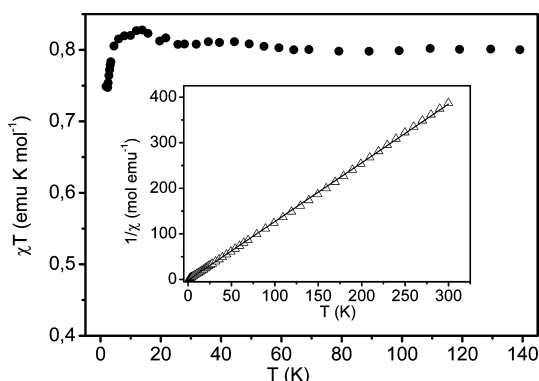


Figure 8. χT vs T plot for complex **2** (full circles) in the 2–140 K range. In the inset the Curie–Weiss plot (empty triangles) over the full temperature range is reported together with the corresponding best fit line obtained with parameters reported in the text.

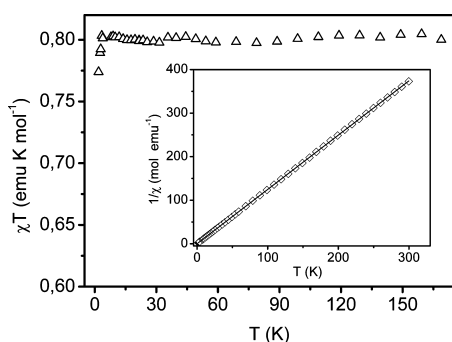


Figure 9. χT vs T plot for complex **3** (empty triangles) in the 2–150 K range. In the inset the Curie–Weiss plot (empty squares) over the full temperature range is reported, together with the corresponding best fit line obtained with parameters reported in the text.

behavior of the three complexes should in principle take into account several steric, structural, and electronic effects, including the differences in the coordination spheres of Cu(II) atoms. A first point to be noted is, however, that neither the magnitude nor the sign of the interaction appear to be related to the Cu...Cu distance, since the interaction is much stronger for **1** (Cu...Cu = 12.30 Å) than for **2** (Cu...Cu = 11.55 Å) and **3** (Cu...Cu = 5.68 Å). Compounds **1** and **3** deserve further attention since both show an intermolecular Cu...N (3.2–3.3 Å) interaction as well as a weak interaction between the beta-diketone ligand and a bipyridine ligand of a different molecule. It is then quite obvious to consider whether magnetic coupling can take effect through these interactions. The local geometry of the involved Cu(II) ions is the same in the two compounds, but while **1** exhibits an antiferromagnetic coupling, **3** has a negligible magnetic interaction. Hence, we exclude that any of these interactions plays a role in the magnetic coupling of the two species. For compound **2**, following the same reasoning, we discard any relevant effect of the bipyridine ligands π ... π stacking on the magnetic exchange coupling. It is then clear that the exchange interaction is essentially transmitted via delocalization through the π -system of the phenyl ring. In aromatic linkers, the spin sign alternates along the linker atoms leading to ferro- or antiferro-magnetic coupling, depending on the number of atoms located between the interacting metal ions because of *spin polarization* mechanism. In such cases, one would expect that the major role is played by a subtle balance between the spin-polarization mechanism,

provided by the bridging π -system, and its relative orientation to the magnetic orbitals of the interacting metal centers.¹⁵ In the case under study, the maximum overlap of the magnetic orbitals of Cu(II) ions ($d_{x^2-y^2}$) with the π -system of the ring is expected when perfect orthogonality of the aromatic plane to the copper–oxygen planes occurs.¹⁶ This would then lead to antiferromagnetic interactions for *ortho* and *para* isomers, while ferromagnetic interactions are expected for the *meta* derivative. On the basis of the above-discussed structural consideration (Figure 5), we can qualitatively explain the magnetic behavior of the three compounds. Compound **1** presents an antiferromagnetic coupling as expected for the *para* isomer because of spin polarization along the aromatic linker. Moreover, the copper ions equatorial planes are close to orthogonality with the phenyl ring leading to a moderate magnetic coupling. At variance, the deviation from orthogonality between the planes becomes larger (Figure 5) for compounds **2** and **3**. As proved by the corresponding Curie–Weiss plots (inset of Figure 8 and 9), the spin polarization effect is still operating leading to ferro- and antiferro-interaction, respectively. However, on the basis of considerations of the orthogonality among planes, this mechanism is expected to be substantially weakened, a fact which might account for the much smaller magnitude of the observed interactions for these two derivatives compared to compound **1**.

CONCLUSIONS

Bis-(3-acetylacetonate)benzene isomers (*para*, *meta*, and *ortho*) behave as highly versatile coordinating ligands that promptly react with Cu(II) ions in simple and designed conditions. The affinity of these ligands for copper ions is so strong that the presence of a base for the deprotonation is not necessary. Three crystalline dimers (**1**–**3**) with an analogue square pyramidal coordination around the Cu(II) ions and the bis β -diketone ligands bridging the metal atoms are readily obtained. Compounds **1** and **3** form supramolecular chains in the solid state because of intermolecular interactions. The three dimeric complexes show antiferromagnetic or ferromagnetic interaction, which is dependent on the position of the two acetylacetonate groups on the aromatic ring because of *spin polarization* mechanism. In addition, differences in the magnitude of the magnetic coupling are also evidenced, and they are correlated to structural parameters. The moderate antiferromagnetic coupling ($J = -3.3 \text{ cm}^{-1}$) observed in compound **1** regardless of the remarkable intermetal distance (Cu...Cu = 12.30 Å) opens intriguing perspectives in the investigation of long distance electron mediated interactions. The chemistry of the bis-(3-acetylacetonate)benzene ligands will be extended to further transition metals, and structure-properties correlations will be studied taking into account steric, structural, and electronic effects, including the differences in the coordination spheres of the different metal ions.

ASSOCIATED CONTENT

Supporting Information

Synthesis, X-ray determination, and refinement details, ligands structure description, additional figures, and crystallographic information files (CIF). This material is available free of charge via the Internet at <http://pubs.acs.org>.

■ AUTHOR INFORMATION

Corresponding Author

*E-mail: marzio.rancan@unipd.it (M.R.), silvio.quici@istm.cnr.it (S.Q.), lidia.armelao@unipd.it (L.A.).

Notes

The authors declare no competing financial interest.

■ ACKNOWLEDGMENTS

We thank Prof. E. Tondello for encouragement and helpful discussions. The research was supported by Italian MIUR through FIRB RBPR05JH2P "Rete" ItaNanoNet, FIRB RBAP114AMK "RINAME", and PRIN 20097X44S7 "Record" Projects, and by University of Padova through Progetto Strategico "HELIOS" and the 2008 Scientific Equipment for Research initiative.

■ REFERENCES

- (1) For selected examples see: (a) Clegg, J. K.; Lindoy, L. F.; Moubarak, B.; Murray, K. S.; McMurtrie, J. C. *Dalton. Trans.* **2004**, 2417. (b) Clegg, J. K.; Gloe, K.; Hayter, M. J.; Kataeva, O.; Lindoy, L. F.; Moubarak, B.; McMurtrie, J. C.; Murray, K. S.; Schilter, D. *Dalton. Trans.* **2006**, 3977. (c) Clegg, J. K.; Li, F.; Jolliffe, K. A.; Meehanc, G. V.; Lindoy, L. F. *Chem. Commun.* **2011**, 47, 6042.
- (2) Olivier, J.-H.; Harrowfield, J.; Ziessel, R. *Chem. Commun.* **2011**, 47, 11176, and references therein.
- (3) Pariya, C.; Sparrow, C. R.; Back, C. K.; Sand, G.; Fronczek, F. R.; Maverick, A. W. *Angew. Chem.* **2007**, 119, 6421.
- (4) (a) Rancan, M.; Armelao, L.; Tondello, E.; Dolmella, A.; Bandoli, G.; Quici, S.; Orlandi, S.; Rizzato, S.; Albinati, A.; Sorace, L.; Gatteschi, D. Abstracts of Papers, p 68. In *Proceedings of the XXVIII Congresso Nazionale SCI Divisione di Chimica Inorganica*; Società Chimica Italiana: Trieste, Italy, September 13–16, 2010. (b) Pariya, C.; Fronczek, F. R.; Maverick, A. W. *Inorg. Chem.* **2011**, 50, 2748.
- (5) Lambert, J. B.; Liu, Z. J. *Chem. Crystallogr.* **2007**, 37, 629.
- (6) Rancan, M.; Dolmella, A.; Seraglia, R.; Orlandi, S.; Quici, S.; Armelao, L. *Chem. Commun.* **2012**, 48, 3115.
- (7) Sheldrick, G. M. *Acta Crystallogr.* **2008**, A64, 112.
- (8) Dolomanov, O. V.; Bourhis, L. J.; Gildea, R. J.; Howard, J. A. K.; Puschmann, H. J. *Appl. Crystallogr.* **2009**, 42, 339.
- (9) Ramirez, F.; Bhatia, S. B.; Patwardhan, A. V.; Smith, C. J. *Org. Chem.* **1967**, 32, 3547.
- (10) Ramirez, F.; Patwardhan, A. V.; Ramanathan, N.; Desai, N. B.; Greco, C. V.; Heller, S. R. *J. Am. Chem. Soc.* **1965**, 87, 543.
- (11) Gianelli, L.; Amendola, V.; Fabbrizzi, L.; Pallavicini, P.; Mellerio, G. G. *Rapid Commun. Mass Spectrom.* **2001**, 15, 2347.
- (12) (a) Kebarle, P.; Ho, Y. *Electrospray Ionization Mass Spectrometry: Fundamentals, Instrumentation and Applications*; Cole, R. B., Ed.; John Wiley & Sons: New York, 1997; (b) Blades, A. T.; Ikononou, M. G.; Kebarle, P. *Anal. Chem.* **1991**, 63, 2109.
- (13) Bleaney, B.; Bowers, K. D. *Proc. R. Soc. London, Ser. A* **1952**, 214, 451.
- (14) (a) Felthouse, T. R.; Duesler, E. N.; Hendrickson, D. N. *J. Am. Chem. Soc.* **1978**, 100, 618. (b) Chaudhuri, P.; Oder, K.; Wiegardt, K.; Gehring, S.; Haase, W.; Nuber, B.; Weiss, J. J. *Am. Chem. Soc.* **1988**, 110, 3657. (c) Bürger, K. S.; Chaudhuri, P.; Wiegardt, K.; Nuber, B. *Chem.—Eur. J.* **1995**, 1, 583. (d) Pardo, E.; Faus, J.; Julve, M.; Lloret, F.; Muñoz, M. C.; Cano, J.; Ottenwaelde, X.; Journaux, Y.; Carrasco, R.; Blay, G.; Fernández, I.; Ruiz-García, R. *J. Am. Chem. Soc.* **2003**, 125, 10770. (e) Paital, A. R.; Wu, A. Q.; Guo, G. G.; Aromí, G.; Ribas-Ariño, J.; Ray, D. *Inorg. Chem.* **2007**, 46, 2947. (f) Ferrando-Soria, J.; Castellano, M.; Yuste, C.; Lloret, F.; Julve, M.; Fabelo, O.; Ruiz-Pérez, C.; Stiriba, S.-E.; Ruiz-García, R.; Cano, J. *Inorg. Chim. Acta* **2010**, 363, 1666. (g) Castellano, M.; Fortea-Pérez, F. R.; Stiriba, S.-E.; Julve, M.; Lloret, F.; Armentano, D.; De Munno, G.; Ruiz-García, R.; Cano, J. *Inorg. Chem.* **2011**, 50, 11279.
- (15) Bencini, A.; Gatteschi, D.; Totti, F.; Sanz, D. N.; Mc Cleverty, J. A.; Ward, M. D. *J. Phys. Chem. A* **1998**, 102, 10545.
- (16) Dul, M.-C.; Ottenwaelde, X.; Pardo, E.; Lescouezec, R.; Journaux, Y.; Chamoreau, L.-M.; Ruiz-García, R.; Cano, J.; Julve, M.; Lloret, F. *Inorg. Chem.* **2009**, 48, 5244.